Suspended magnetic polymer structures fabricated using dose-controlled ultraviolet exposure

Jui-Chang Kuo, Chong-Shuo Li, Hsueh-Chien Cheng, Yao-Joe Yang

Department of Mechanical Engineering, National Taiwan University, Taipei, Taiwan
E-mail: yjy@ntu.edu.tw

Published in Micro & Nano Letters; Received on 17th July 2013; Accepted on 19th July 2013

Presented is a process for fabricating suspended magnetic polymer structures with SU-8 photoresist dispersed Fe_3O_4 nanoparticles. By controlling the exposure doses of ultraviolet (UV) is shown light, floating structures are patterned during the first UV exposure and then the anchor structures are patterned at the second exposure. It is shown that suspended magnetic polymer structures, such as doubly-clamped beams, can be successfully fabricated and released using a single development process. In addition, the functionalities and characteristics of these magnetic doubly-clamped beams are demonstrated and discussed. The resonant frequencies of these structures were measured under a sinusoidal magnetic field at an amplitude of 10.37 mT; the frequencies for structures 5 and 6 mm long were 5.21 and 4.18 kHz, respectively.

1. Introduction: Microelectromechanical systems (MEMS) devices that incorporate magnetic materials have been widely employed in actuators, sensors and microfluidic devices [1–5]. These microdevices can be manipulated magnetically without physical contact between any apparatus and the devices, and they can generally be operated in magnetically transparent media such as air, vacuum and conducting and non-conducting liquids [6–10]. Leong *et al.* [11] proposed a mass-producible, tetherless microgripper that can be moved magnetically, the gripping motion of which can be triggered by temperature. Lee *et al.* [12] developed torsional magnetic microactuators for displacing biological materials in implantable catheters, and these microactuators were found to reduce cellular accumulation significantly. Miller *et al.* [13] proposed a multi-analyte sensing system that uses magnetic microbeads to detect DNA hybridisation; giant magnetoresistance (GMR) magnetoelectronic sensors embedded in the chip were used to detect the magnetic microbeads. Schaller *et al.* [14] developed an electrowetting on dielectric-based microfluidic chip for transporting water droplets with magnetic nanoparticles; they also described measuring the magnetic AC-susceptibility of the sample droplets by using a superconducting quantum interference device (SQUID) gradiometer.

MEMS devices with polymer-based material have several advantages compared with devices that use silicon or metal. For example, structures with polymer-based materials have a low Young's modulus [15], and can therefore achieve larger deformation under an applied force. Polymer-based devices can also be easily fabricated using techniques such as photolithography or micromoulding [16]. Suter *et al.* [17] fabricated microcantilevers by using a photocurable polymer composite with superparamagnetic characteristics, and demonstrated uniform distribution and low particle agglomeration in the photocurable polymer matrix SU-8. Tsai *et al.* [18] characterised the properties of SU-8 polymer microactuators with embedded nickel nanoparticles. Kim *et al.* [19] designed polymeric nanocomposite microactuators driven by programmable heterogeneous magnetic anisotropy; these devices can be moved two- and three-dimensionally by programming the rotational axis of each component. Chung *et al.* [20] developed a magnetic actuator fabrication technique by using magnetic nanoparticles containing an ultraviolet (UV)-curable polymer in a polydimethylsiloxane (PDMS) channel. Using a single exposure step, both the anchored and moving portions of the actuator were fabricated based on selective oxygen inhibition. Nakahara *et al.* [21] presented a self-aligned fabrication process for realising active membranes as microactuators on an SU-8 patterned chip. Gach *et al.* [22] presented transparent magnetic photoresists which can be utilised to form micropallet arrays for cell separation using a magnetic field. Klejwa *et al.* [23] proposed a laser-printing process for creating patterned thin film magnetic-polymer composite microstructures directly on planar silicon substrates. Li *et al.* [24] employed an inexpensive photopatternable magnetic polymer for realising heterogeneous magnetic structures. The proposed polymer comprises neodymium iron boron microparticles dispersed in an UV-curable polymer matrix.

Most of the previous methods developed for fabricating suspended structures require an etching process to remove the sacrificial layer for releasing floating structures. In addition, most of the fabrication processes are relatively complicated and require multiple lithography, etching and deposition steps. In this Letter, we present a simple fabrication process for creating suspended magnetic polymer structures by dose-controlled UV exposure of SU-8 photoresist [25]. Suspended structures, such as doubly-clamped beams, are fully released after a single development process of the photoresist. The structures fabricated using this process offer several advantages: biocompatibility, chemical resistance, thermal stability and low cost. These structures are also suitable for biomedical applications with low-power actuation. In addition, the structure employing superparamagnetic nanoparticles can be manipulated by magnetic fields. We will also present the mechanical characterisation of the fabricated beams.

This Letter is organised as follows: the operational principle and design are presented in Section 2. The proposed fabrication process is described in Section 3. Measured results of the fabricated doubly-clamped beams and the discussions are presented in Section 4. Finally, Section 5 draws the conclusions.

2. Process design and operational principle: Fig. 1 shows the schematic of the doubly-clamped beam fabricated using the proposed process which employs dose-controlled UV exposures. Note that the details of the process can be found in the next Section. The schematic of the doubly-clamped beam is used for describing the corresponding analytical models. Based on the Euler beam assumption, as a magnetic field (H) is applied to the

doi: 10.1049/mnl.2013.0438

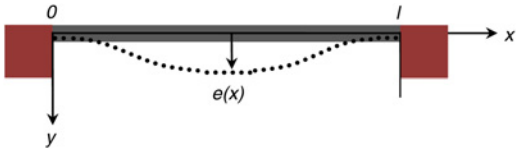

Figure 1 *Schematic of doubly-clamped beam realised by proposed process steps*

structure, the shape of the beam ($e(x)$) can be represented as [26]

$$e(x) = \sum_{n=1}^{\infty} a_n \left(1 - \cos\frac{2n\pi x}{l}\right) \quad (1)$$

where a_n is the amplitude of the mode shape, l is the length of the beam and n is the number of the mode.

Equation (2) is the resonance frequency of the doubly-clamped beam [26, 27]

$$\omega_n = \frac{(n + (1/2))^2 \pi^2}{l^2}\sqrt{\frac{EI}{m}} \quad (2)$$

where ω_n is the resonant frequency of the doubly-clamped beam, E is the Young's modulus of the doubly-clamped beam, A is the cross-sectional area of the beam, I is the moment of inertia and m is the mass of the doubly-clamped beam.

3. Fabrication: Suspended magnetic polymer structures were fabricated using the photo-patternable SU-8 photoresist (SU-8 2050, MicroChem) dispersed with Fe_3O_4 nanoparticles [polyvinylpyrrolidone (PVP)-coated, nanostructured and amorphous]. This magnetic SU-8 photoresist has the machining capability of the photoresist and the functionality of the magnetic material. When coated with PVP, the Fe_3O_4 nanoparticles can be dispersed thoroughly in an SU-8 photoresist [28]. The diameter of the Fe_3O_4 nanoparticles is ~20–30 nm, so the fabricated magnetic structures possess the property of superparamagnetism. The magnetic moment per volume of this superparamagnetic material is higher than that of typical paramagnetic material [17, 18].

The magnetic SU-8 photoresist was first mixed using an ultrasonic agitator at 40 kHz for 2 h to disperse the Fe_3O_4 nanoparticles (at 5, 10 and 15 wt%), and was then mixed using a planetary mixer for 30 min. Finally, the magnetic SU-8 photoresist was degassed in a vacuum chamber to reduce bubbles in the material.

The process parameters of the pure and magnetic SU-8 photoresists were also studied. Fig. 2*a* shows the measured thickness of the SU-8 photoresists at different speeds of the spin-coating; thickness was measured using a surface profiler. Each data point on the curve is the average of five measurements with the same fabrication parameters, and the error bars indicate the maximal and minimal values obtained. As shown in this Figure, the thickness of the SU-8 films decreased as the spin speed increased. Moreover, the magnetic SU-8 photoresists were slightly thicker than pure photoresists at the same spin speed. Fig. 2*b* shows the measured thicknesses of the magnetic SU-8 structures under different UV exposure doses. Higher exposure dose was found to generate a thicker SU-8 film. The magnetic SU-8 photoresist had a lower optical transmittance because of the dispersed magnetic nanoparticles [5, 17] and therefore required, compared with pure SU-8 photoresists, relatively higher UV exposure doses.

Fig. 3 shows the schematics of the steps involved in our proposed fabrication process, which includes two dose-controlled UV exposures of the photoresist for creating suspended magnetic microstructures. Using these steps, we fabricated a suspended magnetic doubly-clamped beam in this Letter. As shown in Fig. 3*a*, the first UV exposure dose was controlled in the depth direction from

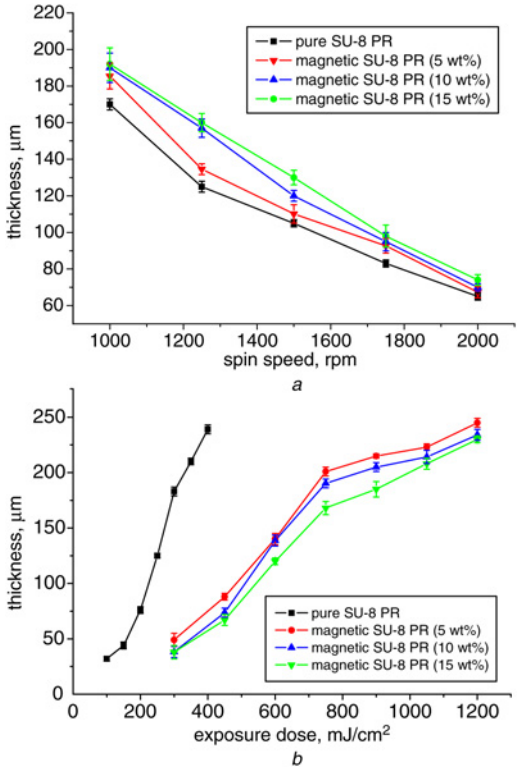

Figure 2 *Measured thickness of SU-8 photoresists at different spin-coating speeds (Fig. 2a), and of thicknesses of magnetic SU-8 structures under various UV exposure doses (Fig. 2b)*

the surface to the substrate, so that the photoresist was patterned for the suspended structure with a specific thickness. The second UV exposure forms the anchors for the suspended structures (Fig. 3*b*), which are released after the photoresist is developed.

Fig. 3*c* shows the fabrication process of the suspended magnetic polymer structure. The SU-8 photoresist was spin-coated on a silicon substrate (Fig. 3*c*(i)); the rotation speed of the spin coater was set at 1000 rpm for obtaining a 160 µm-thick SU-8 photoresist layer (anchor structure). The coated SU-8 photoresist was then soft baked on a hotplate at 65° for 5 min and at 95° for 15 min. The magnetic SU-8 photoresist was spin-coated on the SU-8 photoresist (Fig. 3*c*(ii)); the rotation speed of the spin coater was 1500 rpm for obtaining a magnetic SU-8 photoresist layer (floating structure). The spin-coated SU-8 photoresists were next soft baked on a hotplate at 65° for 5 min and at 95° for 20 min. Fig. 3*c*(iii) shows the first UV exposure for patterning the floating structure by using the first shadow mask with a UV exposure dose of 300 mJ/cm^2. Fig. 3*c*(iv) shows the second UV exposure for patterning the anchors by using the second shadow mask with a UV exposure dose of 1000 mJ/cm^2. After this step, the SU-8 photoresists were baked again (i.e. post-exposure bake) at 65° for 5 min and 95° for 10 min. As shown in Fig. 3*c*(v), the suspended magnetic polymer structure was generated by releasing them through a development process that involved using the SU-8 developer for 10 min with sonication. Finally, the fabricated structure was hard baked at 150° for 15 min.

Figs. 4*a* and 4*b* show the scanning electron microscope (SEM) images of the top and side views of the fabricated magnetic doubly-clamped beams. These beams are 200 µm wide, 5–10 mm long and 40 µm thick.

4. Measurements and discussion: To demonstrate the characteristics of the fabricated magnetic polymer structures, we used a vibrating sample magnetometer for measuring three samples with various magnetic nanoparticle concentrations (5, 10

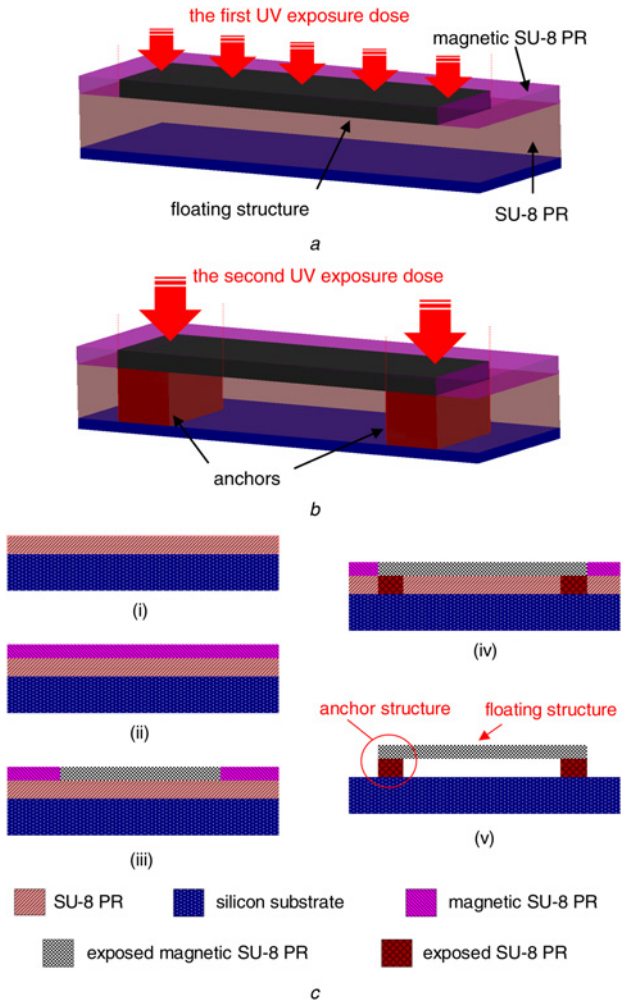

Figure 3 *Schematics of steps in proposed fabrication process, which includes two dose-controlled UV exposures of photoresist for generating suspended magnetic microstructures*
a First UV exposure for patterning floating structures
b Second UV exposure for patterning anchors
c Proposed process for fabricating suspended magnetic polymer structure

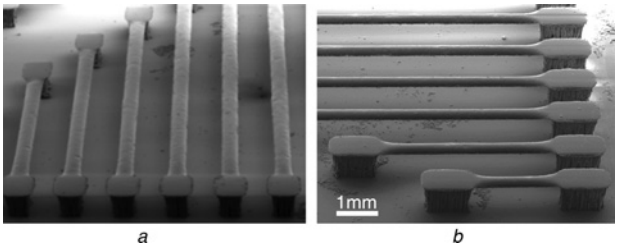

Figure 4 *SEM images of fabricated suspended magnetic polymer structures*
a Top view
b Side view

and 15 wt%). The magnetisation measurements of these three magnetic SU-8 photoresist samples showed that magnetisation was proportional to the Fe_3O_4 concentration (Fig. 5*a*). The remanent magnetisation at zero applied magnetic field was extremely small, indicating the superparamagnetic characteristic of the nanoparticles (because the particle size is smaller than the critical size for superparamagnetism).

Fig. 5*b* shows the experimental setup for measuring the transient displacement and resonance frequency of the magnetic doubly-clamped beams. A function generator and a power amplifier were

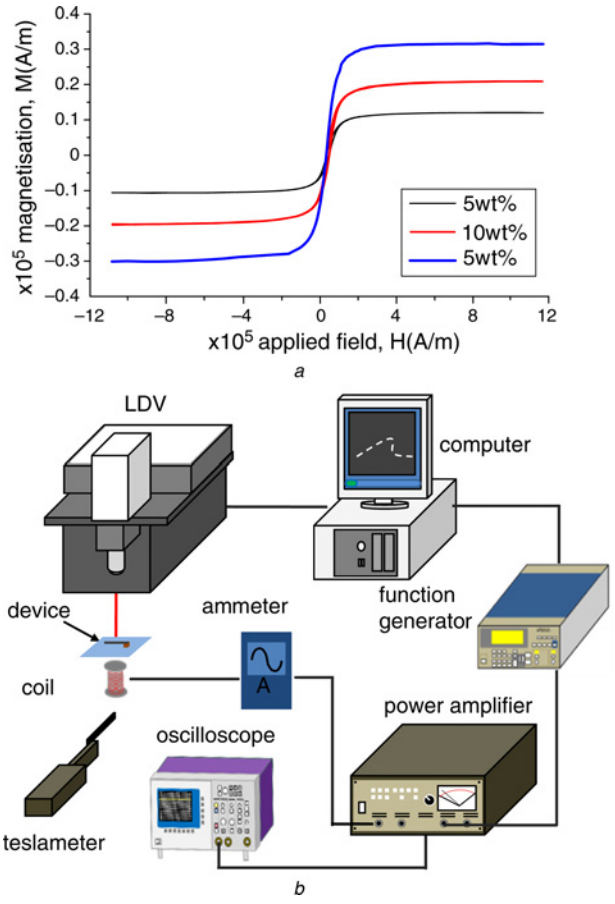

Figure 5 *Magnetisation measurements of magnetic SU-8 photoresists with different Fe_3O_4 concentrations (Fig. 5a), and experimental setup for measuring deformations of fabricated devices (Fig. 5b)*

employed to provide sinusoidal and square input voltages to an external coil, which generates the magnetic fields applied to the doubly-clamped beam. Concurrently, an ammeter was connected in series to measure the current of the circuitry, and a laser Doppler vibrometer was used to measure the displacement of the beam.

Displacements of the central position of the doubly-clamped beams were measured at different amplitudes of the sinusoidal input voltages (Fig. 6*a*). The beams were 10 mm long, 200 µm wide, 40 µm thick and the peak values of the amplified 300 Hz sinusoidal input voltages were 1, 2, 3 and 4 V. Note that the magnetic nanoparticle concentrations of the beams is 15 wt%. The displacement of the centre point of the doubly-clamped beam was linearly dependent on the input voltage signals. The maximal displacement at the centre of the beam is ~60 nm when the amplitude of the sinusoidal driving voltage was 4 V.

During the mentioned measurements, an ammeter and a teslameter were used to measure the AC current in the coil and the magnitude of the vertical magnetic field applied to the doubly-clamped beams. The maximal displacement, the AC current and the vertical magnetic field measured for the four input voltages are shown in Table 1. Fig. 6*b* shows the transient step response of the doubly-clamped beams (6 mm long, 200 µm wide, 40 µm thick and dispersed with 15 wt% magnetic nanoparticles). When the 4 V signal was applied to the coil, the central position of the doubly-clamped beam suddenly deformed downwards and vibrated at its damped frequency of ~4.1 kHz.

The measured frequency responses of the doubly-clamped beams (15 wt% magnetic nanoparticles) under a 10.37 mT sinusoidal magnetic field are shown in Fig. 6*c*. The resonant frequencies of

doi: 10.1049/mnl.2013.0438

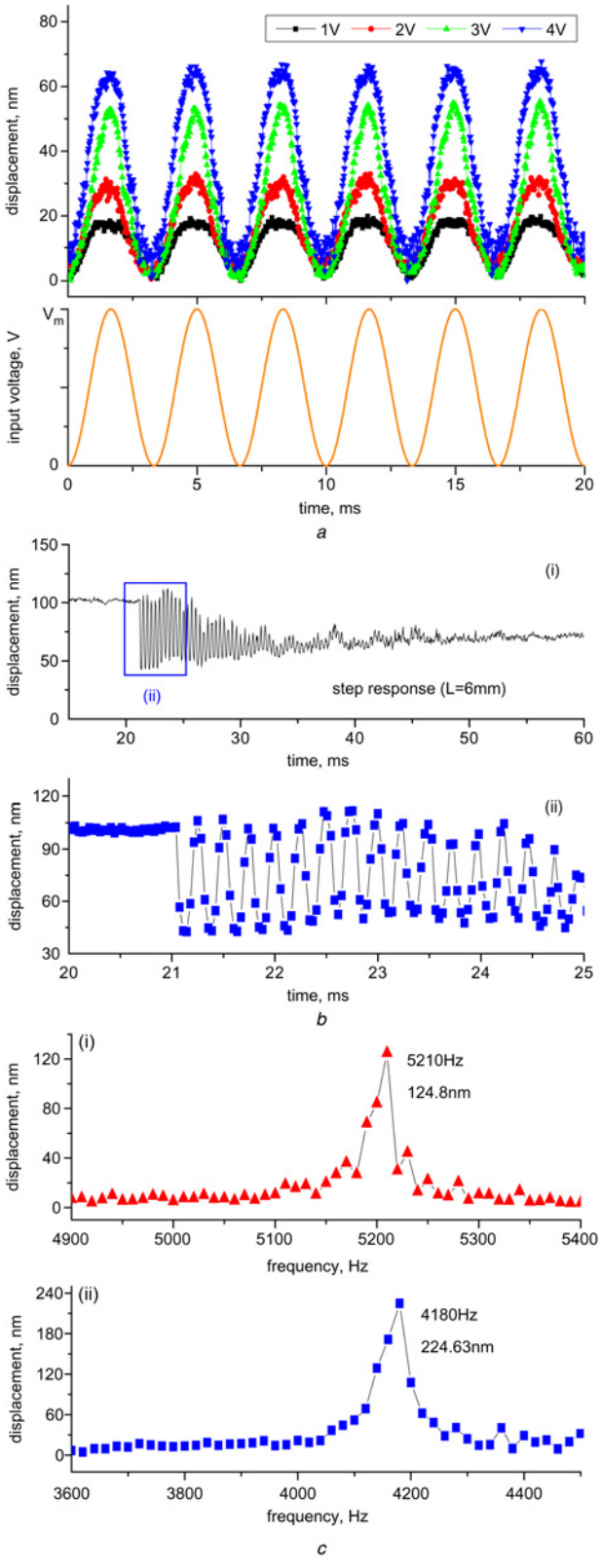

Figure 6 *Measured displacements of central position of doubly-clamped beams at various amplitudes of sinusoidal input voltages (Fig. 6a); transient response of doubly-clamped beam under step input of magnetic field (Fig. 6b); measured frequency responses of doubly-clamped beams ((i)* L = *5 mm, (ii)* L = *6 mm)*

beams 5 and 6 mm long were 5.21 and 4.18 kHz, respectively. The maximal displacement was 124.8 nm for the 5 mm beam and 224.63 nm for the 6 mm beam. The results of these measurements showed that the resonant frequencies increased as the length of the magnetic doubly-clamped beam decreased, and that the longer magnetic doubly-clamped beam produced higher displacement than the shorter beam under the same magnetic field. For the 5 mm beam, the quality factors extracted from the measured results (Fig. 6*c*) is about 104. For the 6 mm beam, the quality factor is about 42. The first-mode ($n = 1$) resonant frequencies estimated using the analytical model of (2) are listed in Table 2. The Young's modulus used in the model is 1.2 GPa, which was measured using a nanoindenter. For the 5 mm beam, the estimated resonant frequency was 5.58 kHz, a discrepancy of ~6.6% compared with the measured result; for the 6 mm beam the estimated resonant frequency was 3.87 kHz, a 8% discrepancy.

Table 1 Measured values of maximal displacements, AC current, vertical magnetic field for four input voltages

V_m, V	Max. displacement, nm	AC current, A	Vertical magnetic field, mT
1	16.44	0.17	5.12
2	32.87	0.34	8
3	55.37	0.56	9.15
4	67.72	0.72	10.37

Table 2 Resonant frequencies estimated using analytical model presented in Section 2

Length of beam, nm	Resonant frequency (analytical), kHz	Resonant frequency (experimental), kHz	Discrepancy, %
5	5.58	5.21	6.61
6	3.87	4.18	8.01

5. Conclusion: This Letter presents a process for fabricating suspended magnetic polymer structures. The proposed process involves employing a polymer composite consisting of SU-8 photoresist dispersed with Fe_3O_4 nanoparticles. Using this process with dose-controlled UV exposure, the floating structures can be patterned at the first exposure and the anchor structures can then be patterned at the second exposure. Suspended magnetic polymer structures, such as doubly-clamped beams, can be fabricated successfully after being released using a single development process. The resonant frequencies of these structures were measured under a sinusoidal magnetic field at an amplitude of 10.37 mT. These frequencies and the maximal displacements for beams 5 and 6 mm long were 5.21 and 4.18 kHz and 124.8 and 224.63 nm, respectively. This Letter demonstrates and discusses the functionalities and characteristics of the magnetic doubly-clamped beams. The magnetic structures fabricated by the proposed process potentially can be employed as the actuating mechanisms for micropumps, magnetic valves and cell manipulation devices.

6. Acknowledgments: The authors thank K.-S. Chen of the National Cheng-Kung University for help on Young's modulus measurement using a nanoindenter. This work was supported in part by the National Science Council, Taiwan (contract no: NSC 100-2221-E-002-075-MY3).

7 References

[1] Zheng X., Zhang X.: 'Opto-mechanical platforms for cell force study', *Micro Nano Lett.*, 2011, **6**, pp. 332–336

[2] Damean N., Parviz B., Lee J., Odom T., Whitesides G.: 'Composite ferromagnetic photoresist for the fabrication of microelectromechanical systems', *J. Micromech. Microeng.*, 2005, **15**, pp. 29–34
[3] Qiao R., Yang C., Gao M.: 'Superparamagnetic iron oxide nanoparticles: from preparations to in vivo MRI applications', *J. Mater. Chem.*, 2009, **19**, pp. 6274–6293
[4] Pirmoradi F., Jackson J., Burt H., Chiao M.: 'On-demand controlled release of docetaxel from a battery-less MEMS drug delivery device', *Lab. Chip*, 2011, **11**, pp. 2744–2752
[5] Suter M., Ergeneman O., Zurcher J., *ET AL.*: 'A photopatternable superparamagnetic nanocomposite: material characterization and fabrication of microstructures', *Sens. Actuators B, Chem.*, 2011, **156**, pp. 433–443
[6] Rodriguez C., Castro E., Martin A., Marin J., Berganza J., Cuevas J.: 'Magnetic poly(styrene/divinylbenzene/acrylic acid)-based hybrid microspheres for bio-molecular recognition', *Micro Nano Lett.*, 2011, **6**, pp. 349–352
[7] Ruan M., Shen J., Wheeler C.B.: 'Latching micromagnetic relays', *J. Microelectromech. Syst.*, 2001, **10**, pp. 511–517
[8] Khoo M., Liu C.: 'Micro magnetic silicone elastomer membrane actuator', *Sens. Actuators A, Phys.*, 2001, **89**, pp. 259–266
[9] Gass J., Poddar P., Almand J., Srinath S., Srikanth H.: 'Superparamagnetic polymer nanocomposites with uniform Fe_3O_4 nanoparticle dispersions', *Adv. Funct. Mater.*, 2006, **16**, pp. 71–75
[10] Horsley D., Davis W., Hogan K., *ET AL.*: 'Optical and mechanical performance of a novel magnetically actuated MEMS-based optical switch', *J. Microelectromech. Syst.*, 2005, **14**, pp. 274–284
[11] Leong T., Randall C., Benson B., Bassik N., Stern G., Gracias D.: 'Tetherless thermobiochemically actuated microgrippers', *Proc. Natl. Acad. Sci. USA*, 2009, **106**, pp. 703–708
[12] Lee S., Lee H., Pinney J., Khialeeva E., Bergsneider M., Judy J.: 'Development of microfabricated magnetic actuators for removing cellular occlusion', *J. Micromech. Microeng.*, 2011, **21**, p. 054006 (12pp)
[13] Miller M., Sheehan P., Edelstein R., *ET AL.*: 'A DNA array sensor utilizing magnetic microbeads and magnetoelectronic detection', *J. Magn. Magn. Mater.*, 2001, **225**, pp. 138–144
[14] Schaller V., Velasco A., Kalabukhov A., *ET AL.*: 'Towards an electrowetting-based digital microfluidic platform for magnetic immunoassays', *Lab. Chip*, 2009, **9**, pp. 3433–3436
[15] Schmid S., Wagli P., Hierold C.: 'Biosensor based on all-polymer resonant microbeams'. Proc. MEMS2009, Sorrento, Italy, 2009, pp. 300–303
[16] Johansson A., Blagoi G., Boisen A.: 'Polymeric cantilever-based biosensors with integrated readout', *Appl. Phys. Lett.*, 2006, **89**, pp. 89–91
[17] Suter M., Ergeneman O., Zurcher J., *ET AL.*: 'Superparamagnetic photocurable nanocomposite for the fabrication of microcantilevers', *J. Micromech. Microeng.*, 2011, **21**, p. 025023 (8pp)
[18] Tsai K., Moayyed M., Candler R., *ET AL.*: 'Magnetic, mechanical, and optical characterization of a magnetic nanoparticle-embedded polymer for microactuation', *J. Microelectromech. Syst.*, 2011, **20**, pp. 65–72
[19] Kim J., Chung S., Choi S., Lee H., Kim J., Kwon S.: 'Programming magnetic anisotropy in polymeric microactuators', *Nat. Mater.*, 2011, **10**, pp. 747–752
[20] Chung S., Kim J., Choi S., Kim L., Kwon S.: 'In situ fabrication and actuation of polymer magnetic microstructures', *J. Microelectromech. Syst.*, 2011, **20**, pp. 785–787
[21] Nakahara T., Hosokawa Y., Terao K., *ET AL.*: 'Self-aligned fabrication process for active membrane made of photosensitive nanocomposite'. Proc. MEMS2012, Paris, France, 2012, pp. 1181–1184
[22] Gach P.C., Sims C.E., Allbritton N.L.: 'Transparent magnetic photoresists for bioanalytical applications', *Biomaterials*, 2010, **31**, pp. 8810–8817. doi:10.1016/j.biomaterials.2010.07.087
[23] Klejwa N., Misra R., Provine J., *ET AL.*: 'Laser-printed magnetic-polymer microstructures'. Transducers, Denver, CO, USA, June 2009, pp. 865–868; doi: 10.1109/SENSOR.2009.5285826
[24] Li H., Flynn T.J., Nation J.C., Kershaw J., Stephens L.S., Trinkle C. A.: 'Photopatternable NdFeB polymer micromagnets for microfluidics and microrobotics applications', *J. Micromech. Microeng.*, 2013, **23**, p. 065002 (7pp), doi:10.1088/0960-1317/23/6/065002
[25] Kuo J.-C., Li C.-S., Yang Y.-J.: 'Suspended magnetic polymer structures fabricated with exposure dose control'. Proc. NEMS2013, Suzhou, China, 2013, pp. 779–782
[26] Senturia S.D.: 'Microsystem design' (Kluwer Academic, 2001)
[27] Abbott J., Ergeneman O., Kummer M., Hirt A., Nelson B.: 'Modeling magnetic torque and force for controlled manipulation of soft-magnetic bodies', *IEEE Trans. Robot.*, 2007, **23**, (6), pp. 1247–1252
[28] Liu H., Ko S., Wu J., *ET AL.*: 'One-pot polyol synthesis of monosize PVP-coated sub-5 nm Fe_3O_4 nanoparticles for biomedical applications', *J. Magn. Magn. Mater.*, 2007, **310**, pp. e815–e817

doi: 10.1049/mnl.2013.0438